

A model for longitudinal and shear wave propagation in viscoelastic media

Thomas L. Szabo, and Junru Wu

Citation: [The Journal of the Acoustical Society of America](#) **107**, 2437 (2000); doi: 10.1121/1.428630

View online: <https://doi.org/10.1121/1.428630>

View Table of Contents: <https://asa.scitation.org/toc/jas/107/5>

Published by the [Acoustical Society of America](#)

ARTICLES YOU MAY BE INTERESTED IN

[Time domain wave equations for lossy media obeying a frequency power law](#)

[The Journal of the Acoustical Society of America](#) **96**, 491 (1994); <https://doi.org/10.1121/1.410434>

[Modified Szabo's wave equation models for lossy media obeying frequency power law](#)

[The Journal of the Acoustical Society of America](#) **114**, 2570 (2003); <https://doi.org/10.1121/1.1621392>

[Ultrasonic Waves in Solid Media](#)

[The Journal of the Acoustical Society of America](#) **107**, 1807 (2000); <https://doi.org/10.1121/1.428552>

[Quantifying elasticity and viscosity from measurement of shear wave speed dispersion](#)


[The Journal of the Acoustical Society of America](#) **115**, 2781 (2004); <https://doi.org/10.1121/1.1739480>

[Causal theories and data for acoustic attenuation obeying a frequency power law](#)

[The Journal of the Acoustical Society of America](#) **97**, 14 (1995); <https://doi.org/10.1121/1.412332>

[Determination of velocity and attenuation of shear waves using ultrasonic spectroscopy](#)

[The Journal of the Acoustical Society of America](#) **99**, 2871 (1996); <https://doi.org/10.1121/1.414880>



CAPTURE WHAT'S POSSIBLE
WITH OUR NEW PUBLISHING ACADEMY RESOURCES

Learn more ➔

AIP
Publishing

A model for longitudinal and shear wave propagation in viscoelastic media

Thomas L. Szabo^{a)}

Agilent Technologies, 3000 Minuteman Road, Andover, Massachusetts 01810

Junru Wu^{b)}

Department of Physics, University of Vermont, Burlington, Vermont 05405

(Received 7 December 1998; accepted for publication 16 February 2000)

Relaxation models fail to predict and explain loss characteristics of many viscoelastic materials which follow a frequency power law. A model based on a time-domain statement of causality is presented that describes observed power-law behavior of many viscoelastic materials. A Hooke's law is derived from power-law loss characteristics; it reduces to the Hooke's law for the Voigt model for the specific case of quadratic frequency loss. Broadband loss and velocity data for both longitudinal and shear elastic types of waves agree well with predictions. These acoustic loss models are compared to theories for loss mechanisms in dielectrics based on isolated polar molecules and cooperative interactions. © 2000 Acoustical Society of America. [S0001-4966(00)04705-6]

PACS numbers: 43.35.Bf, 43.35.Cg, 43.35.Mr [HEB]

BACKGROUND

In many instances, loss data taken from infrasound to ultrasound frequencies (Bamber, 1986; White, 1965; Collins and Lee, 1956; Szabo, 1995) follow a simple frequency, f , power law with constants α_0 and α_1 ,

$$\alpha(f) = \alpha_0 + \alpha_1 |f|^y, \quad (1)$$

where y is a positive number usually less than 2 and most often, α_0 is set to zero. Absorption data for $\alpha(f)$ are shown in Fig. 1 for a wide range of viscoelastic materials and frequency ranges. The longitudinal wave loss of bovine liver (Polhammer, 1973), shown with an exponent $y=1.3$ for 1–100 MHz, is typical of materials that are in the commonly occurring range, $1 \leq y \leq 2$. Human myocardium (Kudo *et al.*, 1997), once thought to follow a Voigt model (Ahuja, 1979), also falls in this range for y at ultrasound frequencies, as do many other tissues (Goss *et al.*, 1979; Bamber, 1986; Duck, 1990). At lower frequencies, many plastics, including data given later in this paper, aromatic polyurethanes (Guess and Cambell, 1995), and noncrosslinked polymers (Bagley and Torvik, 1983), fall into this range of exponent y . At very high ultrasound frequencies, single crystalline materials such as yttrium indium garnet (YIG), follow a quadratic power law with shear wave loss less than that of the longitudinal wave. Perhaps the most striking examples of the absorption following a frequency power law are those in seismology literature. White (1965) summarizes absorption data that as linear with frequency for six decades of frequency. Data extracted from his summary for two types of granite in Fig. 1 indicate this linear dependence from 140 Hz to 2.2 MHz. Note here shear wave loss is greater than that of a longitudinal wave, a more typical result.

Effects of absorption are usually described by a material transfer function in the frequency domain of the form, $\exp\{-\alpha(f) + i\beta(f)z\}$, where z is the distance of propagation from a source. Usually β is taken to mean $\beta = 2\pi f/V_0$, where V_0 is a constant speed of sound in the medium. In order to completely describe the effects of absorption in a causal way, velocity dispersion, $V(f)$, must be included; this means that $\beta(f)$ is a more complicated function of frequency. We present methods for determining $\beta(f)$ from data to complete the description for absorption of the power law type in Sec. I.

The loss characteristics of Fig. 1 are not predicted by a classic relaxation theory such as the Voigt dashpot model (Herzfeld and Litovotz, 1959; Kinsler *et al.*, 1982; Bamber, 1986; Auld, 1990) which has the well-known attenuation and velocity characteristics illustrated in Fig. 2. The basis of this model is a modified Hooke's law which has an added viscous term relating stress T (a second rank tensor) to the time derivative of strain S (also a second rank tensor),

$$T = c:S + \eta: \frac{\partial S}{\partial t}, \quad (2)$$

in dyadic notation (see the Appendix), where c is an elastic stiffness constant fourth rank tensor and η is a viscosity constant fourth-rank tensor.

Many attempts have been made to make relaxation models fit the types of data illustrated by Fig. 1. When no resonance is visible in absorption versus frequency data, an assumption is often made that a resonance occurs at a very high frequency beyond the measurement range, so that a low frequency approximation can be applied. From Fig. 2(a), at low frequencies, the absorption α has a frequency-squared dependence for absorption. For these frequencies, the speed of sound is nearly constant at low frequencies [in Fig. 2(b), the propagation factor divided frequency, β/ω is inverse velocity]. These characteristics do not match the type of data in Fig. 1.

^{a)}Electronic mail: tom_szabo@agilent.com

^{b)}Electronic mail: jwu@zoo.uvm.edu

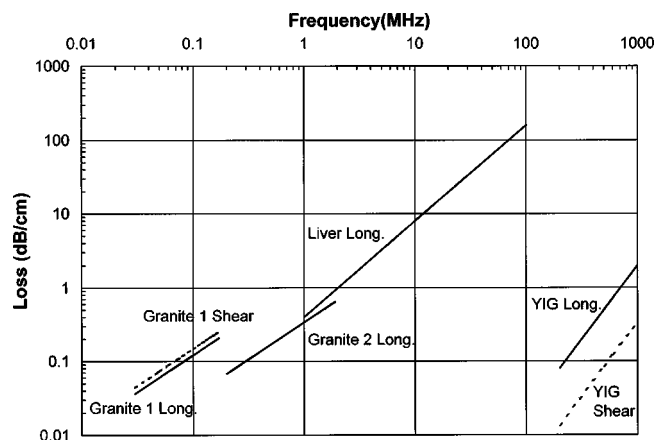


FIG. 1. Data for shear and longitudinal wave loss which show power-law dependence over four decades of frequency.

Others have suggested that, over a specified range of frequencies, a combination of relaxation functions can be used to approximate a power law. White (1965) discusses the attempts made to match data. Postma (1958) indicated such approximations were possible, and Horton (1959) achieved a reasonable fit to the linear loss of Pierre shale over a range of frequencies by using four relaxation constants. In principle, data can be fitted by a sum of relaxation constants over a frequency range as described by Tschoegel (1989). The application of multiple relaxation constants to match a desired power-law variation over a restricted frequency range will result in a time response consisting of a superposition of exponentially decaying relaxation constants, quite unlike the time response obtained for the power-law case in Secs. II and III. Models have also been proposed involving either a distribution or continuum of relaxation constants (Bamber,

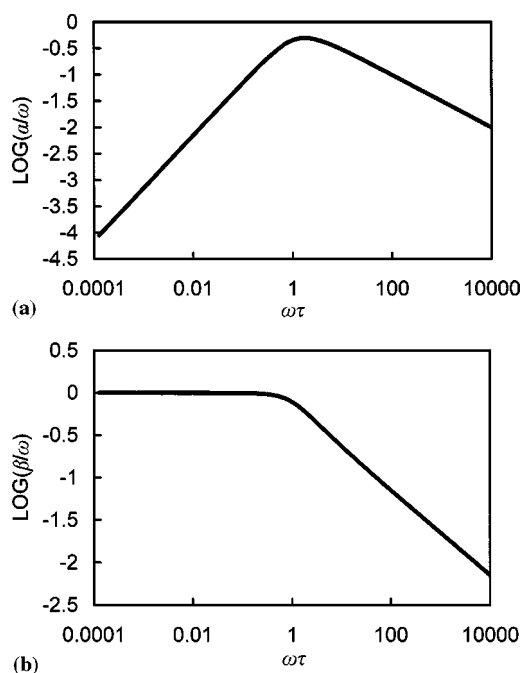


FIG. 2. (a) Absorption α divided by angular frequency ω vs angular frequency ω times τ for the Voigt dashpot model. Loss peak at $\omega_p = 1/\tau$, where τ is relaxation time. (b) Excess dispersion β divided by angular frequency ω vs angular frequency ω times τ .

1986; Aki and Richards, 1980; Nachman *et al.*, 1990; Szabo, 1993).

Ferry (1980, p. 59) wrote that “although an arbitrary set of parameters would suffice to predict macroscopic behavior, it would not be unique and would be of little value for theoretical interpretation. This difficulty can be avoided, however, by substituting continuous spectra.” White (1965) remarked that it is doubtful that these approaches would match linear frequency dependence of loss data observed over six decades of frequency. These attempts to fit data mask the possibility that these losses could depend on fundamental natural mechanisms other than relaxation phenomena. This topic is discussed in Sec. IV.

INTRODUCTION

Is there another paradigm better matched to observed losses in viscoelastic media than relaxation phenomena? This study extends previous work for fluids (Szabo, 1993, 1994) to describe losses in viscoelastic media based on a frequency power law, Eq. (1), such as all the cases depicted in Fig. 1. Elastic wave equations describe lossless propagation. New wave equations which contain an extra loss term appropriate for viscoelastic media are derived in the Appendix.

The model developed here is based on the assumption that the loss per wavelength is small, about $\alpha/\lambda \leq 0.6$, as explained in Sec. I and the end of the Appendix. A consequence of the smallness approximation is that the model becomes slightly less accurate at extremely high frequencies. For example, for loss of longitudinal YIG of Fig. 1, a conservative estimate of a high-frequency limit is 3.8×10^{12} Hz, which is well beyond the practical measurement range for this material. As the wavelength approaches the scale of material structure at these extremely high frequencies, other loss mechanisms (not in this theory) are expected to dominate.

Power-law data, as indicated by Fig. 1 and by data for liquids (Szabo, 1995) tend to preserve their unique frequency dependence over an extremely wide range. This model holds for any reasonable positive value of the exponent y and has been shown to agree well with data with values from $y=0.5$ to 2 (Szabo, 1995; He, 1998a, 1998b, 1999).

A consequence of this model is a more comprehensive Hooke's law in which the relation between stress and strain includes a convolution operator $r(S,t)$ which replaces the derivative term in Eq. (2)

$$T = c:S + \eta:r(S,t). \quad (3)$$

A direct relationship between this law and absorption and dispersion is part of the derivation in the Appendix. The Hooke's laws in Eqs. (2) and (3) are illustrated symbolically in Fig. 3. Specific forms of these laws are in Sec. II. There, we shall show that Hooke's law from the Voigt model is a special instance of Eq. (3).

As mentioned earlier, phase velocity dispersion is a causal by-product of absorption. General relations between absorption and velocity dispersion for viscoelastic media (Sec. I) apply even when the underlying physical causes of loss are unknown and the loss characteristic and/or velocity dispersion are acquired through measurement. These rela-

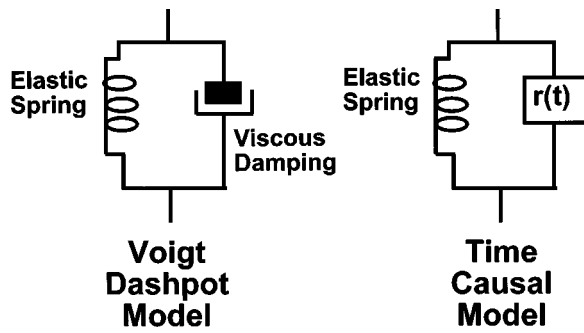


FIG. 3. Left: the schematic representation of Hooke's law for Voigt dashpot model. Right: representation of time causal model with function $r(t)$ replacing the dashpot as the viscous element.

tions will be shown to agree well with both longitudinal and shear wave loss and dispersion data in Sec. III.

I. ABSORPTION AND VELOCITY DISPERSION

For a medium with absorption losses, the speed of sound is dispersive in the most general case. A material transfer function (MTF) for a viscoelastic medium is

$$MTF(\omega) = \exp[\gamma_M(\omega)z], \quad (4)$$

where a complex wave number or propagation factor γ can be written as a function of ω , angular frequency, $\omega = 2\pi f$, for each elastic mode M (here, $M=S$ denotes a shear mode and $M=L$, longitudinal mode),

$$\gamma_M(\omega) = -\alpha_M(\omega) + i\beta_M(\omega), \quad (5a)$$

$$\gamma_M(\omega) = -\alpha_M(\omega) + i[\beta_{OM}(\omega) + \beta_{EM}(\omega)], \quad (5b)$$

where V_{OM} is a constant speed of sound for each mode, $\beta_{OM} = \omega/V_{OM}$. $\beta_{EM}(\omega)$ is an excess dispersion term needed to satisfy causality so that for each mode, the overall velocity varies with frequency as

$$V_M(\omega) = \omega/\beta_M(\omega) = [1/V_{OM} + \beta_{EM}(\omega)/\omega]^{-1}. \quad (6)$$

The absorption power law is recast for viscoelastic modes,

$$\alpha_M = \alpha_{OM} + \alpha_{1M}|\omega|^y, \quad (7)$$

where α_{OM} is a constant and

$$\alpha_{1M} = \frac{\eta_{IJ}}{2c_{IJ}V_{OM}}, \quad (8)$$

in which, in terms of the abbreviated subscripts of the Appendix, $M=S$, $IJ=44$ for the shear case; and for the longitudinal case, $M=L$, and $IJ=11$. For example, as shown in the Appendix, if $y=2$, there is no dispersion, or $\beta_{EM}=0$, and $\alpha_M = \alpha_{1M}\omega^2$. For loss with values of y which are not even integers, $\beta_{EM}(\omega) \neq 0$.

These results provide the structure needed for determination of wave equations and solutions for the general power-law case of attenuation, Eq. (7), where y can be any positive, finite (reasonably valued) value and for the derivation of a more comprehensive form of Hooke's law, Eq. (3). The necessary derivations are outlined in the Appendix and they draw on a time-domain statement of causality used in an earlier work on losses in fluids, Szabo (1994) and a smallness approximation (see the end of the Appendix). Dispersion is found to be of the following forms:

for y as an even integer or noninteger,

$$\beta_{EM}(\omega) = \alpha_{1M} \tan(\pi y/2) \omega |\omega|^{y-1}, \quad (9)$$

and for y as an odd integer,

$$\beta_{EM}(\omega) = -(2/\pi) \alpha_{1M} \omega^y \ln|\omega|. \quad (10)$$

Versions of these equations more appropriate for velocity data are the following:

For y as an even integer or noninteger,

$$1/V_M(\omega) = 1/V_M(\omega_0) - \alpha_{1M} \tan(\pi y/2) [|\omega|^{y-1} - |\omega_0|^{y-1}], \quad (11)$$

in which $V_M(\omega_0)$ is the speed of sound at a reference frequency ω_0 . For y as an odd integer,

$$1/V_M(\omega) = 1/V_M(\omega_0) - (2\alpha_{1M}\omega^{y-1}/\pi)(\ln|\omega| - \ln|\omega_0|). \quad (12)$$

II. HOOKE'S LAW FOR POWER-LAW ABSORPTION

From these expressions for attenuation and dispersion, explicit solutions for $r(t)$ for a more comprehensive Hooke's

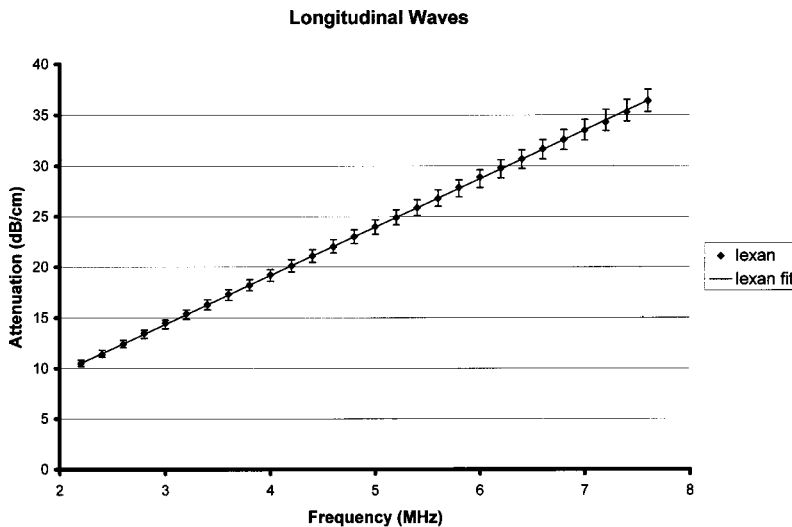


FIG. 4. Absorption loss data with error bars and frequency power law for longitudinal waves in Lexan.

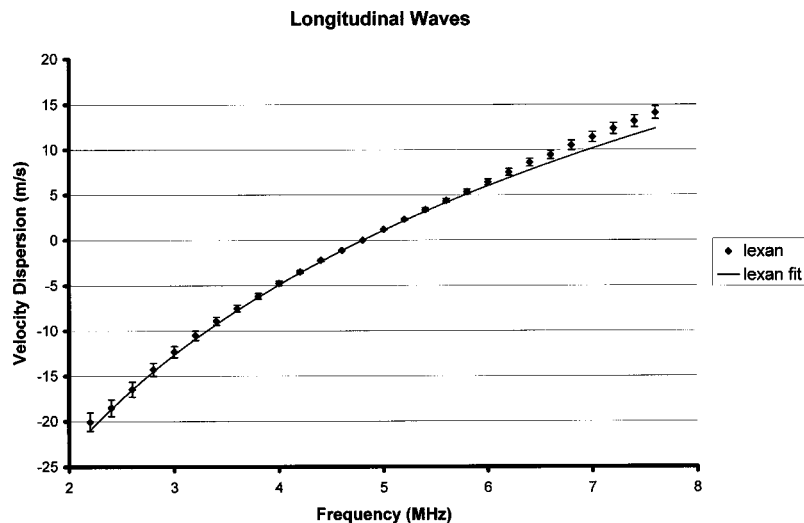


FIG. 5. Velocity dispersion predicted from time causal model compared to velocity data referenced to 4.8-MHz value with error bars for longitudinal waves in Lexan.

law, Eq. (3), are given in the Appendix. Different forms of this Hooke's law depend on the value of y . For y as an even integer,

$$T(t) = c:S(t) - (-1)^{y/2} \eta: \frac{\partial^{y-1} S(t)}{\partial t^{y-1}}, \quad (13)$$

and for the common case, $y=2$, Eq. (13) reduces to the Voigt model, Eq. (2). When y is an odd integer,

$$T(t) = c:S(t) + \eta: \left[\frac{2}{\pi} (y-1)! (-1)^{(y+1)/2} \frac{H(t)}{t^y} * S(t) \right], \quad (14)$$

in which $H(t)$ is the step function (Bracewell, 1968).

For the important case of $y=1$,

$$T(t) = c:S(t) + \eta: \left[\frac{-2}{\pi} \frac{H(t)}{t} * S(t) \right]. \quad (15)$$

Finally, for the most general case of y as a noninteger,

$$T(t) = c:S(t) + \eta: \left[\frac{-2}{\pi} \Gamma(y) \sin(\pi y/2) \frac{H(t)}{|t|^y} * S(t) \right], \quad (16)$$

where Γ is a gamma function. For y as a noninteger which is slightly greater than 1, $y = 1 + \varepsilon$,

$$T(t) \approx c:S(t) + \eta: \left[\frac{-2}{\pi} \frac{H(t)}{|t|^{1+\varepsilon}} * S(t) \right]. \quad (17)$$

With the help of generalized functions, the Fourier transform of the general stress Eq. (3) provides stress as a function of frequency,

$$T(\omega) = c:S(\omega) + \eta:R(S, \omega). \quad (18)$$

For the commonly used Voigt model, the Fourier transform of Eq. (2) leads to the following:

$$T(\omega) = c:S(\omega) + i\omega \eta: S(\omega). \quad (19)$$

Equation (19) provides the basis for the concept of a complex elastic constant, $c + i\omega \eta$ (Auld, 1990) for materials fitting a Voigt model. A complex elastic constant would not be appropriate for power-law absorption in general because of the more complicated relation that is expressed by Eq. (18).

Bagley and Torvik (1983) developed an empirical model for a Hooke's law based on the relation

$$T(\omega) = E_0:S(\omega) + (i\omega \eta)^{y-1} E_1:S(\omega), \quad (20)$$

where the constants E_0 and E_1 are determined empirically from data. Using fractional derivatives, they derived a model

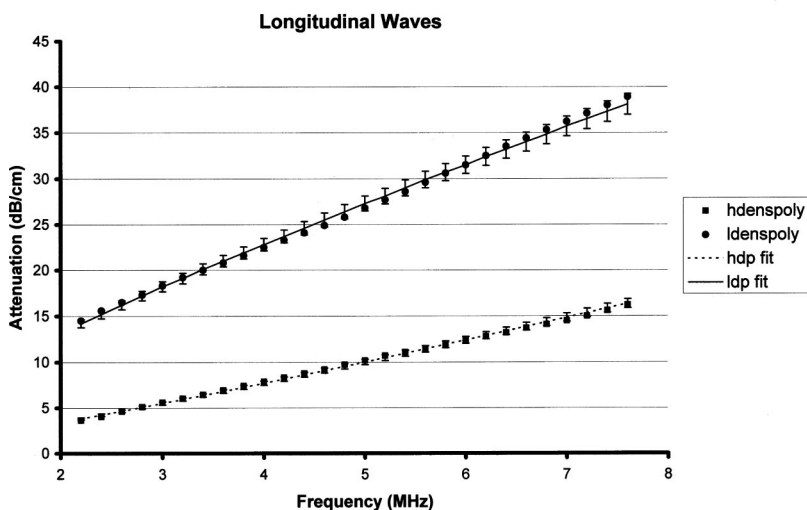


FIG. 6. Absorption loss data with error bars and frequency power law for longitudinal waves in low-density polyethylene and high-density polyethylene.

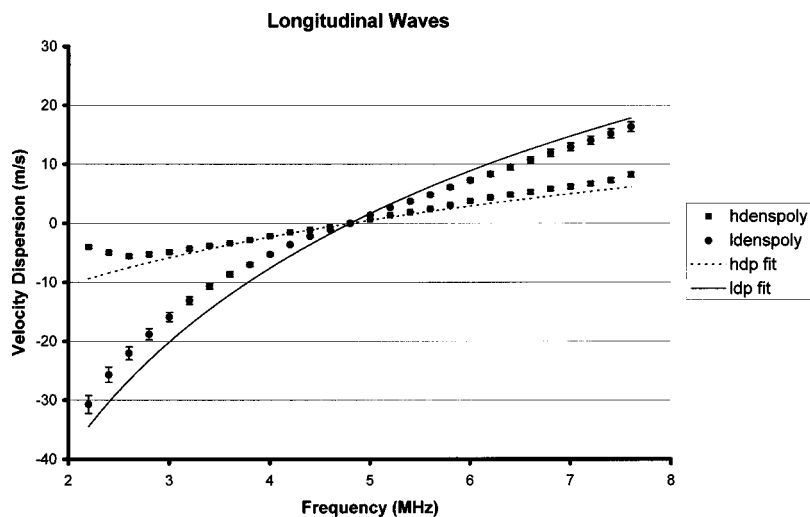


FIG. 7. Velocity dispersion predicted from time causal model compared to velocity data referenced to 4.8-MHz value with error bars for longitudinal waves in low-density polyethylene and high-density polyethylene.

for the range $1 < y < 2$. Their time-domain version of Eq. (20) is similar in form to Eq. (16) for the noninteger values of y in that it depends on a step function divided by t raised to a power of y ; however, it is missing the explicit dependence on y in Eq. (16) which is traceable to absorption. The sine term in Eq. (16) indicates that the factor should be maximum at $y=1$ (or odd integers) and diminish as y approaches 0 or 2, a characteristic that is seen in absorption data (Szabo, 1995). The experimental support for the empirical model is based on fits to complex moduli of the form of Eq. (20) for materials with $y \sim 1.5$, so it is not possible to determine how their data vary with y . The important cases of integral values of y , Eqs. (13) and (14) in the present model, are not covered by Bagley and Torvik's empirical model. Related approaches are discussed in Tschoegl (1989).

III. DATA

A. Experiments

For a given data set, the determination of α_{0M} , α_{1M} and y can be found from a least-squares power-law fit. Conversely, if a power-law fit were applied to velocity data, the absorption could be determined; however, this approach has been found to be less reliable experimentally. Typically, the velocity change with frequency is small, on the order of one part in 10^3 , so that it is more difficult to measure than attenuation (He, 1998b).

The shear and longitudinal wave data were obtained by the broadband substitution method. This technique, described in detail elsewhere (Wu, 1996), provides a means of determining both attenuation and phase velocity simulta-

neously over a broad bandwidth. In brief, the transmitted pulse between two broadband transducers in a water tank is recorded and digitized; then, a sample is inserted between them and the waveform transmitted through the specimen is also digitized. A complex spectrum is obtained from the test sample waveform and divided by the complex spectrum of the reference water waveform to calculate the attenuation and velocity of the sample. Angular rotation of the sample is used to cause complete mode conversion to obtain the shear wave characteristics. Data are corrected for impedance discontinuities at the sample interfaces by Fresnel equations.

B. Discussion

Longitudinal data are plotted in Figs. 4 and 5 for Lexan (a commercial name of a polymer plastic). The presentation of the data is the following: absorption data points are shown in Fig. 4 along with a least-squares power-law fit; second, the speed of sound data is plotted along with the velocity predicted from the absorption fit and Eq. (12) in Fig. 5. For Lexan, the longitudinal attenuation fit is a nearly linear fit to frequency; the velocity change is logarithmic. Similar results are given for two types of polyethylene in Figs. 6 and 7, where the absorption is no longer linear with frequency and Eq. (11) is used. Detailed coefficients and velocities are summarized in Tables I and II. Data were taken at room temperature (22 °C). Error bars in the plots indicate the variation for both the attenuation and velocity data as well as the estimated error in the velocity prediction.

Shear wave data in Figs. 8–11 are different in several ways from the longitudinal data for these materials. The data for these plastics, even after the usual correction for impedance discontinuities at the sample interfaces, indicate that shear wave absorption is nearly an order of magnitude (in dB/cm) greater than the longitudinal cases. For shear waves,

TABLE I. Absorption coefficients (dB/(MHz)^y-cm) and exponential powers y .

Material	Longitudinal α_{1L}	Longitudinal y	Shear α_{1S}	Shear y
Lexan	4.783	1.001	41.84	0.695
Low density polyethylene	7.577	0.796	28.64	0.815
High density polyethylene	1.522	1.171	22.80	0.950

TABLE II. Reference speed of sound @4.8 MHz ($\times 10^3$ m/s).

Material	Longitudinal	Shear
Lexan	2.195	0.943
Low-density polyethylene	2.566	1.273
High-density polyethylene	2.380	0.987

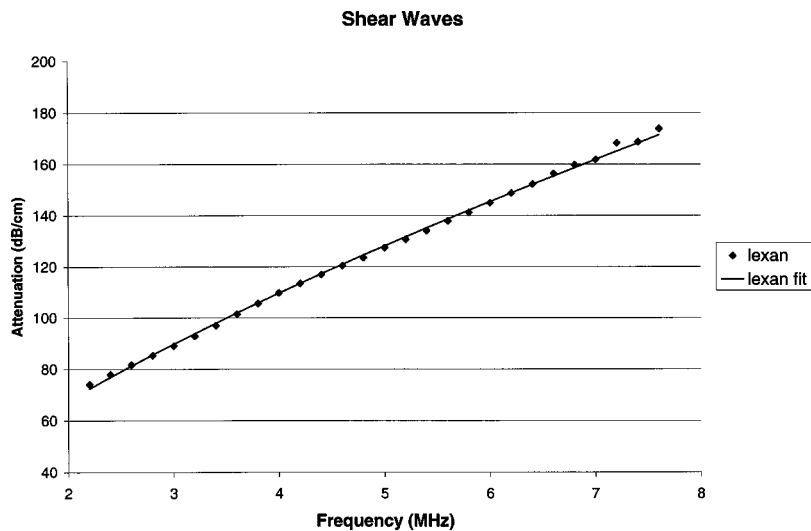


FIG. 8. Absorption loss data with error bars and frequency power law for shear waves in Lexan.

the absorption coefficient α_{0S} is usually nonzero, unlike the longitudinal absorption for these materials. Factors contributing to higher shear wave losses are the lower values of shear wave velocities and shorter wavelengths which lead to more loss per wavelength.

The relative magnitude of shear to longitudinal mode loss depends on material structure. Ferry (1980, pp. 34–37) identifies eight types of polymer structures. For example, polyethylenes fall into a cross-linked category of highly crystalline polymers. In a single-crystal rigid solid (nonpolymer), however, shear wave absorption can be less than longitudinal loss as illustrated by Fig. 1 for YIG.

IV. DISCUSSION

The dominance of the relaxation model for losses in acoustics, as originally derived by Stokes and Kirchhoff for fluids, is matched by a similar situation in electromagnetics where the Debye model has held an analogous position (Jonscher, 1977). The Debye model, originally formulated for noninteracting charged dipoles in a viscous medium, had been the main paradigm for explaining dielectric loss mechanisms. The real, X' , and imaginary susceptance, X'' , for this model, plotted in Fig. 12, are similar to absorption, α/ω , and

dispersion, β/ω , in the acoustic relaxation model of Fig. 2. Both the viscoelastic model and the Debye models are based on independent relaxation events.

Jonscher (1977), in examining dielectric losses for many solids over several decades of frequency, concluded that a fractional frequency power law was “the universal dielectric response.” Later, Hill and Jonscher (1983) developed a more general susceptance model that included a resonance and reduced to different fractional power laws at frequencies above and below the loss peak. They derived their model based on configurational quantum-mechanical tunneling and local fluctuations. Their empirical model is a Gaussian hypergeometric function of normalized frequency, ω/ω_p , where ω_p is the loss peak frequency, and empirically determined indices m and n (similar in function to y of present model), both less than 1. Well below ω_p , this function is close to a frequency raised to a fractional power m ; far above ω_p , it reduces to frequency raised to a fractional power $n-1$. Furthermore, the short-time transition time behavior is proportional to t^{-n} and long time behavior falls as $t^{-(1+m)}$.

In contrast, for acoustic waves in viscoelastic media, the frequency exponent is most often not fractional, but has been found to vary from 0 to 2. Longitudinal mode absorption

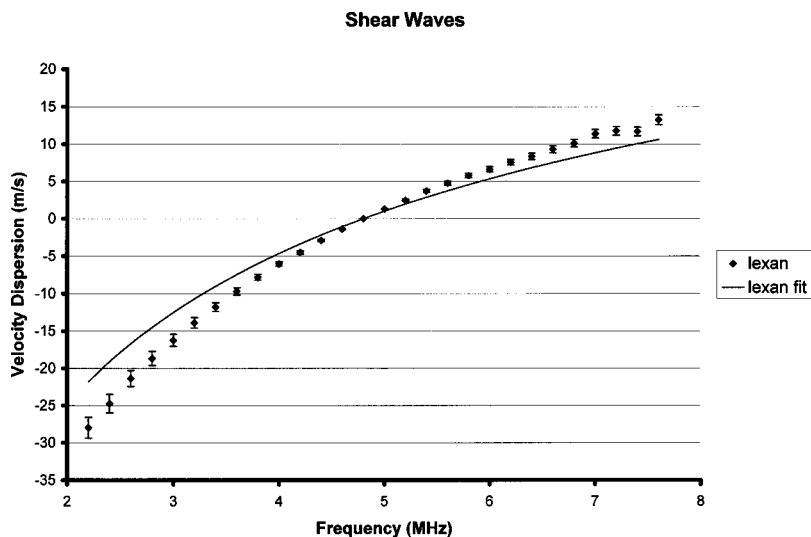


FIG. 9. Velocity dispersion predicted from time causal model compared to velocity data referenced to 4.8-MHz value with error bars for shear waves in Lexan.

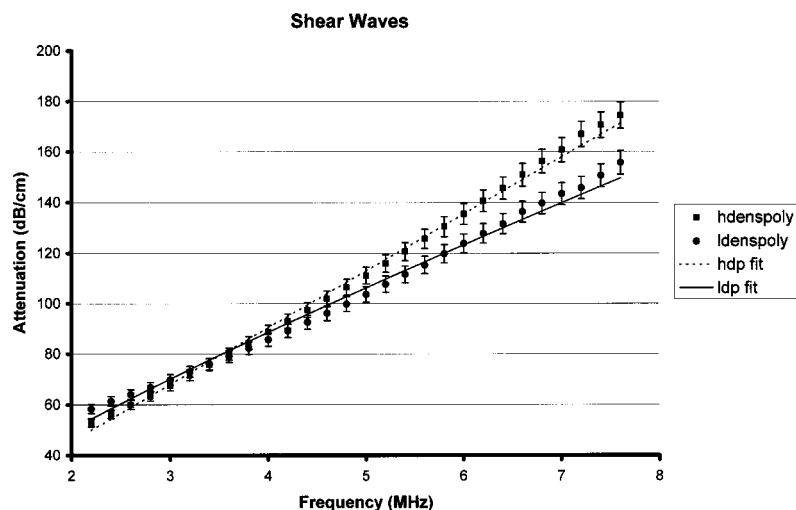


FIG. 10. Absorption loss data with error bars and frequency power law for shear waves in low-density polyethylene and high-density polyethylene.

obeys a power law with an exponent most frequently in the range of $1 < \gamma < 2$ for a large number of materials, both fluid and solid [Duck (1990); Zeqiri (1988); Bamber (1986); Szabo (1993, 1994, 1995); O'Donnell (1981), He (1998a, 1998b, 1999)]. For the shear wave losses in this work, $\gamma < 1$. In the present model, the function $r(t)$ varies inversely with a power of t like the transition times of the Hill and Jonscher dielectric model. This time dependence is in contrast with that of the relaxation model $\exp(-\omega\tau)$. Despite the fact that the acoustic model is for propagating waves, whereas the dielectric theory is for dynamic nonpropagating losses, there are differences as well as similarities.

Hill and Jonscher (1983) explained that their many-body interaction approach accounted for cooperative interactions in solids, and they obtained excellent agreement with data for a wide range of solids. If many-body interactions are occurring for acoustic and elastic waves, the appropriate underlying physical mechanisms are different than the dielectric case. For the plastic materials measured in this study, an extensive body of knowledge exists on the viscoelastic properties of polymers. Ferry (1980), in his text on polymers, distinguishes the character of polymers from the local viscous effects occurring in the deformation of hard solids, "In a polymer, on the other hand, each flexible threadlike mol-

ecule pervades an average volume much greater than atomic dimensions and is continually changing the shape of its contour as it wriggles and writhes with its thermal energy." Complicated interactions between macromolecules include entanglements, branching and cross-linking. In these cases, isolated relaxation mechanisms for acoustic losses seem an unlikely explanation for many materials, just as the isolated polar molecules of the Debye model fail in explaining measured dielectric losses. Bagley and Torvik (1983) and Ferry (1980) have derived macromolecular theories for specific cases. More work is necessary to uncover physical principles which cause the observed absorption to occur for any specific type of material; the role of cooperative interactions appears to be a promising direction for further understanding.

V. CONCLUSIONS

In summary, a comprehensive model accounting for absorption losses of the frequency power-law type has been presented in both time-domain and frequency-domain versions. In general, wave equations for these kinds of loss include convolution operators for both absorption and dispersion. Only for the simple cases of constant loss with

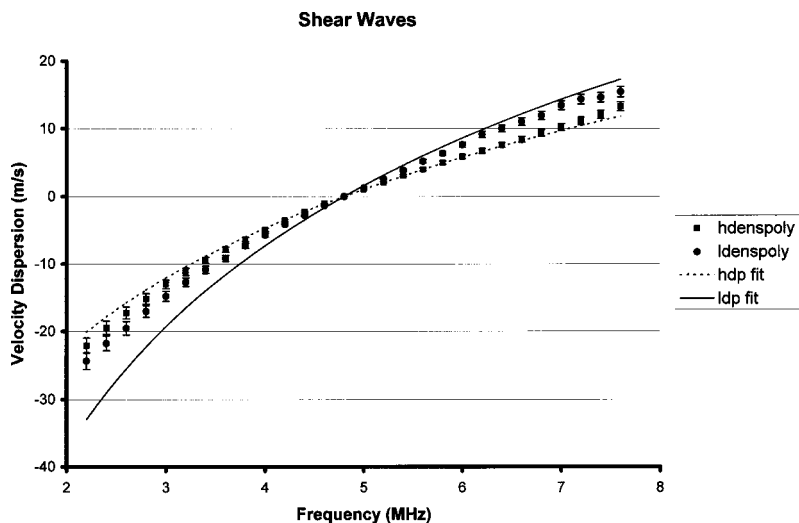


FIG. 11. Velocity dispersion predicted from time causal model compared to velocity data referenced to 4.8-MHz value with error bars for shear waves in low-density polyethylene and high-density polyethylene.

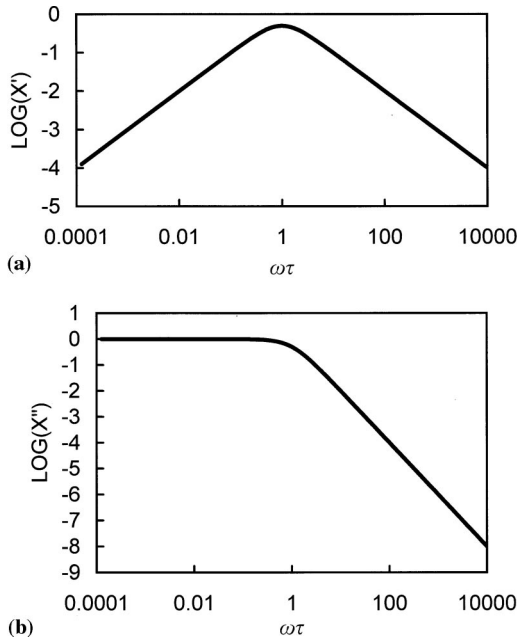


FIG. 12. (a) Real susceptibility X' vs angular frequency ω times τ for the Debye model. Loss peak at $\omega_p = 1/\tau$, where τ is relaxation time. (b) Imaginary susceptibility X'' vs frequency.

frequency or frequency-squared loss do the wave equations reduce to familiar derivative operators for absorption. A consequence of the model is a more comprehensive Hooke's law which reduces to the Voigt model Hooke's law under a low-frequency approximation. Data for losses of shear waves are consistent with the model presented and are much greater than those for longitudinal waves.

APPENDIX: DERIVATION OF LOW FREQUENCY APPROXIMATION OF VOIGT DASHPOT WAVE EQUATION

To derive our model, we follow the steps and the dyadic abbreviated subscript tensor notation used by Auld (1990) for the wave equation of the Voigt model. A particle velocity vector is defined by

$$v = \frac{\partial u}{\partial t}, \quad (\text{A1})$$

where u is a particle displacement vector. The strain-velocity relation is

$$\frac{\partial S}{\partial t} = \nabla_s v. \quad (\text{A2})$$

In order to find wave equations and solutions for the general power-law case of attenuation, Eq. (7), where y can be any positive, finite (reasonably valued) number, a more comprehensive form of Hooke's law is needed

$$T = c:S + \eta:r(S, t), \quad (\text{A3})$$

where c and η are stiffness and viscosity tensors, respectively, S is strain (a second-rank tensor) and in which $r(S, t)$ is yet to be determined. Except for Eq. (A3), the following steps are like those in Auld (1990):

(1) Differentiate Eq. (A3) with respect to time.

(2) Substitute relation (A2) in (A3) to obtain an expression in terms of v .

(3) Differentiate the equation of motion,

$$\nabla \cdot T = \rho \frac{\partial v}{\partial t} - F \quad (\text{A4})$$

(in which ρ is density and F is an applied force, a second-rank tensor) with respect to time and substitute the result for $\partial T / \partial t$ to obtain a wave equation,

$$\nabla \cdot c : \nabla_s v + \nabla \cdot \eta : r(\nabla_s v) = \rho \frac{\partial^2 v}{\partial t^2} - \frac{\partial F}{\partial t}. \quad (\text{A5})$$

In the case of a Voigt solid, $r(S, t) = \partial S / \partial t$, so that for a plane wave propagating along the z axis of an isotropic medium, Eq. (A5) breaks down into two separable modified wave equations for shear and longitudinal waves, respectively,

$$c_{44} \frac{\partial^2 v_x}{\partial z^2} + \eta_{44} \frac{\partial^3 v_x}{\partial z^2 \partial t} = \rho \frac{\partial^2 v_x}{\partial t^2}, \quad (\text{A6})$$

and

$$c_{11} \frac{\partial^2 v_z}{\partial z^2} + \eta_{11} \frac{\partial^3 v_z}{\partial z^2 \partial t} = \rho \frac{\partial^2 v_z}{\partial t^2}. \quad (\text{A7})$$

Phase velocities are defined as longitudinal, $V_L = \sqrt{c_{11}/\rho}$ and shear, $V_S = \sqrt{c_{44}/\rho}$. A solution of the form

$$v_M(z, \omega) = v_{OM}(0, \omega) e^{-i\omega t + \gamma z}, \quad (\text{A8})$$

in which M denotes shear or longitudinal mode, $M = S$ or L , ω is angular frequency, $\omega = 2\pi f$, and γ is the wave number or propagation factor as defined by Eq. (5), can be substituted in Eqs. (A6) and (A7) to obtain the wave-number dispersion relations used to calculate the curves of Fig. 2 for the Voigt model. When the loss per wavelength is small, the smallness approximation $(\alpha \bar{\lambda}_0)^2 \ll 1$, where $\bar{\lambda}_0 = V_{OM}/\omega$, can be applied to Eqs. (A6) and (A7). As shown in Szabo (1993, 1994), this criteria is equivalent to applying a plane wave approximation to the small viscosity terms in the above equations,

$$\frac{\partial v}{\partial t} = -\frac{1}{V} \frac{\partial v}{\partial z}, \quad (\text{A9})$$

therefore, Eqs. (A6) and (A7) become

$$\frac{\partial^2 v_x}{\partial z^2} - \frac{1}{V_S^2} \frac{\partial^2 v_x}{\partial t^2} + \frac{\eta_{44}}{c_{44} V_S^2} \frac{\partial^3 v_x}{\partial t^3} = 0, \quad (\text{A10})$$

$$\frac{\partial^2 v_z}{\partial z^2} - \frac{1}{V_L^2} \frac{\partial^2 v_z}{\partial t^2} + \frac{\eta_{11}}{c_{11} V_L^2} \frac{\partial^3 v_z}{\partial t^3} = 0. \quad (\text{A11})$$

This completes the low frequency approximation of the Voigt model.

In order to derive a more general viscoelastic wave equation, we return to the wave equation containing r , Eq. (A5), which, under the smallness approximation, leads to the counterparts of Eqs. (A10) and (A11) for the isotropic case

$$\frac{\partial^2 v_x}{\partial z^2} - \frac{1}{V_S^2} \frac{\partial^2 v_x}{\partial t^2} + \frac{\eta_{44}}{c_{44} V_S^2} \frac{\partial^2 r(v_x)}{\partial t^2} = 0, \quad (\text{A12})$$

$$\frac{\partial^2 v_z}{\partial z^2} - \frac{1}{V_L^2} \frac{\partial^2 v_z}{\partial t^2} + \frac{\eta_{11}}{c_{11} V_L^2} \frac{\partial^2 r(v_z)}{\partial t^2} = 0. \quad (\text{A13})$$

These last two equations can be represented by the general form

$$\frac{\partial^2 v}{\partial z^2} - \frac{1}{V_{0M}^2} \frac{\partial^2 v}{\partial t^2} - L_\gamma^* \frac{\partial^2 v}{\partial t^2} = 0, \quad (\text{A14})$$

where $L_\gamma(t)$ is a propagation operator. Equations of the same form as Eq. (A14) have been solved for frequency power-law attenuation (Szabo, 1993, 1994). The propagation operator is based on the constraint that causality imposes on Eqs. (A12)–(A14). This constraint, often expressed as a Kramers–Kronig relation, requires that the excess dispersion and attenuation be a Hilbert transform of each other

$$\beta_{EM}(\omega) = \frac{-1}{\pi \omega} * [-\alpha_{1M}(\omega)]. \quad (\text{A15})$$

The extra absorption term α_{0M} is a constant with frequency; therefore, dispersion does not depend on it. Two drawbacks of Eq. (A15) are that the attenuation must be known at all frequencies to determine the dispersion, and that the convolution diverges for values of $y \geq 1$. Appropriate convergent forms of the Kramers–Kronig relations can, however, be found by the method of subtractions and they will satisfy the Paley–Wiener theorem. Through the use of generalized functions, Szabo (1993, 1994) has derived a time causal counterpart of Eq. (A15)

$$L_{\beta_{EM}}(t) = -\text{sgn}(t) * L_\alpha(t), \quad (\text{A16})$$

where $\text{sgn}(t)$ is a signum function (Bracewell, 1968) and $L_{\beta_{EM}}$ and β_{EM} as well as L_α and α_{1M} are Fourier transform pairs. The overall propagation operator can be written as

$$L_\gamma(t) = L_\alpha(t) + iL_{\beta_{EM}}(t) = 2H(t)L_\alpha(t), \quad (\text{A17})$$

where $H(t)$ is the step function (Bracewell, 1968).

The function $r(t)$ can be found from the results previously derived for L_γ by equating Eqs. (A12) and (A13) to Eq. (A14)

$$-L_\gamma^* v = \frac{\eta_{IJ}}{c_{IJ} V_{0M}^2} \frac{\partial^2 r(v)}{\partial t^2} = \frac{2\alpha_{0M}}{V_{0M}} \frac{\partial^2 r(v)}{\partial t^2}. \quad (\text{A18})$$

The explicit results for $r(t)$ depend on whether y is an even, $r(t) = r_e(t)$, or an odd integer, $r(t) = r_o(t)$, or a noninteger $r(t) = r_{ni}(t)$. For y as an even integer,

$$r_e(t) = -(-1)^{y/2} \frac{\partial^{y-1}}{\partial t^{y-1}}. \quad (\text{A19})$$

Note for $y=2$, $r_e(t) = \partial/\partial t$ and so Eq. (3) becomes Eq. (2). For y as an odd integer,

$$r_o(t) = \frac{2}{\pi} (y-1)! (-1)^{(y+1)/2} \frac{H(t)}{t^y}. \quad (\text{A20})$$

For y as a noninteger,

$$r_{ni}(t) = \frac{-2}{\pi} \Gamma(y) \sin(\pi y/2) \frac{H(t)}{|t|^y}. \quad (\text{A21})$$

The above results are valid for a wide frequency range determined by the smallness approximation. The smallness approximation is $(\alpha \bar{\lambda}_0)^2 \ll 1$, where $\bar{\lambda}_0 = V_{0M}/\omega$. For absorption of the form of Eq. (1), a conservative upper-frequency limit f_{LIM} can be estimated (Szabo, 1993, 1994) by setting $\alpha \bar{\lambda}_0 = 0.1$ and solving for f

$$f_{\text{LIM}} = 0.1/(\alpha_{1M} 2\pi V_{0M})^{1/(y-1)}. \quad (\text{A22})$$

In most practical cases, this frequency far exceeds the finite bandwidth of acoustic waveforms of interest. In addition, values of attenuation at very high frequencies usually imply extremely high and unmeasurable values of loss. For example, the upper-frequency limit for the longitudinal YIG loss of Fig. 1 is 3.8×10^{12} Hz, corresponding to a loss of 2.9×10^7 dB/cm. For this conservative condition, $\alpha \bar{\lambda}_0 = 0.1$, the binomial expansion error for the propagation factor is 5×10^{-6} .

- Ahuja, A. S. (1979). "Tissue as a Voigt body for the propagation of ultrasound," *Ultrason. Imaging* **1**, 136–143.
- Aki, K., and Richards, P. G. (1980). *Quantitative Seismology* (Freeman, San Francisco), Vol. 1, Chap. 5.
- Auld, B. A. (1990). *Acoustic Fields and Waves in Solids*, 2nd ed. (Krieger, Malabar, FL), Vol. 1, Chap. 3.
- Bagley, R. L., and Torvik, P. J. (1983). "A theoretical basis for the application of fractional calculus to viscoelasticity," *J. Rheol.* **27**, 201–210.
- Bamber, J. C. (1986). *Physical Principles of Medical Ultrasonics*, edited by C. R. Hill (Wiley, Chichester), pp. 118–199.
- Bracewell, R. N. (1978). *The Fourier Transform and its Applications* (McGraw-Hill, New York).
- Collins, F., and Lee, C. C. (1956). "Seismic attenuation characteristics from pulse experiments," *Geophysics* **1**, 16–40.
- Duck, F. A. (1990). *Physical Properties of Tissue* (Academic, New York).
- Ferry, J. D. (1980). *Viscoelastic Properties of Polymers* (Wiley, New York), pp. 1–33.
- Goss, S. A., Frizzell, L. A., and Dunn, F. (1979). "Ultrasonic absorption and attenuation in mammalian tissues," *Ultrasound Med. Biol.* **5**, 181–186.
- Guess, J. F., and Campbell, J. S. (1995). "Acoustic properties of some biocompatible polymers at body temperature," *Ultrasound Med. Biol.* **21**, 273–277.
- He, P. (1998a). "Simulation of ultrasound pulse propagation in lossy media obeying a frequency power law," *IEEE Trans. Ultrason. Ferroelectr. Freq. Control* **45**, 114–125.
- He, P. (1998b). "Determination of ultrasonic parameters based on attenuation and dispersion measurements," *Ultrason. Imaging* **20**, 275–287.
- He, P. (1999). "Experimental verification of models for determining dispersion from attenuation," *IEEE Trans. Ultrason. Ferroelectr. Freq. Control* **46**, 706–714.
- Herzfeld, K. F., and Litovitz, T. A. (1959). *Absorption and Dispersion of Ultrasonic Waves* (Academic, New York).
- Hill, R. M., and Jonscher, A. K. (1983). "The dielectric behavior of condensed matter and its many-body interpretation," *Contemp. Phys.* **24**, 71–110.
- Horton, C. W. (1959). "A loss mechanism for the Pierre shale," *Geophysics* **24**, 667–680.
- Jonscher, A. K. (1977). "The universal dielectric response," *Nature (London)* **267**, 673–679.
- Kinsler, L. E., Frey, A. R., Coppens, A. B., and Sanders, J. V. (1982). *Fundamentals of Acoustics*, 3rd ed. (Wiley, New York).
- Kudo, N., Kamataki, T., Yamamoto, K., Onozuka, H., Mikami, T., Kitabatake, A., Ito, Y., and Kanda, H. (1997). "Ultrasound attenuation measurement of tissue in frequency range 2.5–40 MHz using a multi-resonance transducer," 1997 Proc. IEEE Ultrasonics Symp., 1181–1184.
- Nachman, A. I., Smith, J. F. III, and Waag, R. C. (1990). "An equation for acoustic propagation in inhomogeneous media with relaxation losses," *J. Acoust. Soc. Am.* **88**, 1584–1595.

- O'Donnel, M., Jaynes, E. T., and Miller, J. G. (1981). "Kramers–Kronig relationship between ultrasonic attenuation and velocity," *J. Acoust. Soc. Am.* **69**, 696–701.
- Polhammer, J. D., Edwards, C. A., and O'Brien, W. D. (1981). "Phase insensitive ultrasonic attenuation coefficient determination for fresh bovine liver over an extended frequency range," *Med. Phys.* **8**, 692–694.
- Postma, G. W. (1958). "Changes of shape of seismic impulses in inhomogeneous viscoelastic media," *Geophys. Prospect.* **6**, 438–455.
- Szabo, T. L. (1993). "Linear and nonlinear acoustic propagation in lossy media," Ph.D. thesis, University of Bath, U.K.
- Szabo, T. L. (1994). "Time domain wave equations for lossy media obeying a frequency power law," *J. Acoust. Soc. Am.* **96**, 491–500.
- Szabo, T. L. (1995). "Causal theories and data for acoustic attenuation obeying a frequency power law," *J. Acoust. Soc. Am.* **97**, 14–24.
- Tschoegl, N. W. (1989). *Phenomenological Theory of Linear Viscoelastic Behavior* (Springer, New York).
- White, J. E. (1965). *Seismic Waves Radiation, Transmission and Attenuation* (McGraw-Hill, New York).
- Wu, J. (1996). "Determination of velocity and attenuation of shear waves using ultrasonic spectroscopy," *J. Acoust. Soc. Am.* **99**, 2871–2875.
- Zeqiri, B. (1988). "An intercomparison of discrete-frequency and broadband techniques for the determination of ultrasonic attenuation," *Physics in Medical Ultrasound*, edited by D. H. Evans and K. Martin (IPSM, London), pp. 27–35.